

# Optimization techniques for the estimation of the thickness and the optical parameters of thin films using reflectance data

**S. D. Ventura**

Institute of Mathematics, Statistics and Computer Science, State University of Campinas - UNICAMP, 13083-970 Campinas, SP, Brazil

**E. G. Birgin**

Institute of Mathematics and Statistics, University of Sao Paulo, 05508-090 Sao Paulo, SP, Brazil

**J. M. Martínez**

Institute of Mathematics, Statistics and Computer Science, State University of Campinas - UNICAMP, 13083-970 Campinas, SP, Brazil

**I. Chambouleyron**<sup>1</sup>

Institute of Physics, State University of Campinas - UNICAMP, 13083-970 Campinas, SP, Brazil

## Abstract

The present work considers the problem of estimating the thickness and the optical constants (extinction coefficient and refractive index) of thin films from the spectrum of normal reflectance  $R$ . This is an ill-conditioned highly under-determined inverse problem. The estimation is done in the spectral range where the film is not opaque. The idea behind the choice of this particular spectral range is to compare the film characteristics retrieved from transmittance  $T$  and from reflectance data.

In the first part of the paper a compact formula for  $R$  is deduced. The approach to deconvolute the  $R$  data is to use well known information on the dependence of the optical constants on photon energy of semiconductors and dielectrics and to formulate the estimation as a nonlinear optimization problem. Previous publications of the group on the subject provide the guidelines for designing the new procedures. The consistency of the approach is tested with computer generated thin films and also with measured  $R$  and  $T$  spectral data of an a-Si:H film deposited onto glass. The algorithms can handle satisfactorily the problem of a poor photometric accuracy in reflectance data, as well as a partial linearity of the detector response.

The results on *gedanken* films and on a-Si:H indicate a very good agreement between expected and retrieved values.

**Keywords:** Optical constants, thin films, reflectance, optimization, numerical algorithms.

---

<sup>1</sup>Author to whom correspondence should be addressed; electronic mail: ivanch@ifc.unicamp.br

# I INTRODUCTION

The optical properties of most thin films depend on deposition techniques and deposition conditions. As many advanced electronic and optical devices require the knowledge of these properties, it is important to develop methods able to extract, with a high degree of precision, the real properties of a deposited film as well as its thickness. For such purpose, the easiest available optical data are the transmittance ( $T$ ) and/or the reflectance ( $R$ ) spectra. In previous publications we considered the problem of retrieving –from transmittance data only– the optical constants [index of refraction  $n(\lambda)$  and absorption coefficient  $\alpha(\lambda)$ ] and the thickness ( $d$ ) of an optical coating deposited onto a transparent substrate. As known, the solution is not unique, this being a highly underdetermined ill-posed inverse-problem (see [1]). To overcome this difficulty we developed two methods: *i*) a pointwise *constrained* optimization approach [2] and, *ii*) a pointwise *unconstrained* optimization approach (PUMA) [3, 4, 5] that proved to be effective in retrieving the true properties of *gedanken* and of real semiconductor films. In these methods the difference between the measured and the calculated transmittance is minimized introducing, with *ad-hoc* procedures, some prior knowledge of the physically meaningful solution. These optimization algorithms proved to be highly reliable for films having a thickness in excess of  $\approx 100$  nm. Recently, we extended the applicability of PUMA to the retrieval of the optical constants and the thickness of very thin amorphous semiconductor films. The new approach, called Functional Form Minimization (FFM), allows us to solve the inverse optical engineering problem for films  $30 \text{ nm} \gtrsim d \gtrsim 100 \text{ nm}$  thick.[6, 7]

Briefly, the proposed approaches consist in imposing constraints that restrict the variability of  $\alpha(\lambda)$  and of  $n(\lambda)$ . Therefore, the estimation problem takes the form:

$$\text{Minimize } \sum_{\lambda} [\text{Predicted Data}(\lambda) - \text{Measured Data}(\lambda)]^2 \quad (1)$$

$$\text{subject to Physical Constraints.} \quad (2)$$

In PUMA [3] the physical constraints are handled in such a way that the final problem turned out to be unconstrained and solved by means of an efficient large-scale minimization method (see [8]). As said, the use of PUMA allows us to retrieve the optical constants and the thickness of both *gedanken* and real amorphous semiconductor films with  $d \gtrsim 100$

nm (see [3, 4]). However, the degree of underdetermination of the estimation problem increases as the thickness of the film decreases, in the  $d \rightarrow 0$  limit (no film at all) all possible  $n(\lambda), \alpha(\lambda)$  parameters give the same functional value in (1).

As a consequence, the mathematical inversion of the transmittance data of very thin films ( $d < 100$  nm) requires more severe constraints in (2). In the Functional Form Minimization approach [6, 7], instead of stating explicitly the constraints for each wavelength value, a functional form is suggested for  $\alpha(\lambda)$  and  $n(\lambda)$  so that the new unknowns are not the values of the optical constants but the (small number of) coefficients of the functional forms. In terms of (2) this represents a severe restriction in the domain of (1). As in the case of PUMA, an appropriate algebraic manipulation allows us to reduce the system of equations to an unconstrained, or box-constrained, optimization problem that can be solved using well established algorithms. In this way it is possible to retrieve the optical properties of real amorphous semiconductor films as thin as 30 nm (see [6]). The method can be extended without difficulty to other homogeneous films like epitaxial crystalline and organic thin layers.

The present contribution is an extension of the above mentioned research. We now consider and solve the inverse optical problem of retrieving the properties of *gedanken* and real films using reflectance data only. The consistency of the retrieval is verified in each case comparing the optical characteristics of the film obtained from reflectance data with those retrieved independently from the transmittance spectrum of the same film. The comparison considers some computer generated films reported in previous publications [3, 7]. As the consistency test can be performed only in the spectral region where transmittance and reflectance data exist simultaneously, the mathematical inversion being presented here includes only the spectral reflectance region where there is some transmittance. Hence, the physical constraints and/or the functional forms imposed to the optical constants in the reflectance spectra under consideration are the same as those used in the treatment of the transmittance data. As a consequence, the retrieval process is not complete because it does not take full advantage of the information contained in the high photon energy region of the reflectance spectrum. The treatment of  $R$  data in the high photon energy spectrum is the subject of a coming publication.

As in the case of the mathematical inversion of a transmittance spectrum, we want to estimate the optical properties of the film using only reflectance data. For each wavelength,

the equation

$$\text{Theoretical Reflectance} = \text{Measured Reflectance} \quad (3)$$

has three unknowns  $d$ ,  $n(\lambda)$ ,  $\alpha(\lambda)$  and only  $d$  is repeated for all values of  $\lambda$ . The under-determination can be overcome incorporating some prior knowledge of the behavior of the functions  $n(\lambda)$ ,  $\alpha(\lambda)$  so that only physically meaningful estimated parameters are allowed. The results show that both  $T$  and  $R$  sets of data can be treated satisfactorily.

The theoretical reflectance of the *air/film/thick substrate/air* structure is first deduced in the next section.

## II REFLECTANCE MODEL

We consider a thin film deposited on a thick transparent substrate. The formulae giving the transmittance as a function of the wavelength  $\lambda$  (see, for example, [9]) are:

$$T = \text{Transmittance} = \frac{Ax}{B - Cx + Dx^2} \quad (4)$$

where

$$A = 16s(n^2 + \kappa^2) \quad (5)$$

$$B = [(n + 1)^2 + \kappa^2][(n + 1)(n + s^2) + \kappa^2] \quad (6)$$

$$C = [(n^2 - 1 + \kappa^2)(n^2 - s^2 + \kappa^2) - 2\kappa^2(s^2 + 1)]2 \cos \varphi - \kappa[2(n^2 - s^2 + \kappa^2) + (s^2 + 1)(n^2 - 1 + \kappa^2)]2 \sin \varphi \quad (7)$$

$$D = [(n - 1)^2 + \kappa^2][(n - 1)(n - s^2) + \kappa^2] \quad (8)$$

$$\varphi = 4\pi nd/\lambda, \quad x = \exp(-\alpha d), \quad \alpha = 4\pi\kappa/\lambda. \quad (9)$$

For future use, we also define the photon energy  $h\nu = E(\text{eV}) = 1240/\lambda(\text{nm})$ . In refs. (4-9),  $d$  is the thickness of the film,  $s$  and  $n$  are the index of refraction of the substrate and of the film, respectively,  $\alpha$  is the absorption coefficient and  $\kappa$  is the (dimensionless) extinction coefficient.

To the authors knowledge, a closed compact formula for the reflectance of the *air / film / thick / substrate / air* structure as a function of wavelength has not been reported. In this section the theoretical reflectance of the structure is deduced, the meaning of the

symbols being the same as in (4)–(9).

Let the system of four layers *air / film / substrate / air* be labeled with the numbers 0,1,2,3 and let the light arrive from the film side. We say that  $\tilde{n}_\nu$  is the complex index of refraction of the layer  $\nu$  and  $L$  is the position of the third interface, separating the substrate from the air. We know (see [1]) that the reflected energy is given by

$$R(\lambda) = \left| \frac{M_{21}}{M_{22}} \right|^2 \quad (10)$$

where

$$M = A_3 (D_2 A_2) (D_1 A_1) \in \mathbb{R}^2 \quad (11)$$

$$D_\nu = \begin{bmatrix} \exp(-i2\pi\tilde{n}_\nu d_\nu/\lambda) & 0 \\ 0 & \exp(i2\pi\tilde{n}_\nu d_\nu/\lambda) \end{bmatrix} \quad (12)$$

for  $\nu = 1, 2$ , and

$$A_\nu = \frac{1}{2\tilde{n}_\nu} \begin{bmatrix} \tilde{n}_\nu + \tilde{n}_{\nu-1} & \tilde{n}_\nu - \tilde{n}_{\nu-1} \\ \tilde{n}_\nu - \tilde{n}_{\nu-1} & \tilde{n}_\nu + \tilde{n}_{\nu-1} \end{bmatrix} \quad (13)$$

for  $\nu = 1, 2, 3$ . In refs. [10, 11], the reflectance is given by forms similar to (10). For one film, the simpler configuration is with the layers *air/film/substrate* (the first and last layers being semi-infinite). However, this leads us to the practical problem of measuring the reflectance inside the substrate. In refs. [12, 13, 14, 15, 16], the retrieval is done either considering a semi-infinite substrate or, alternatively, a four-layered system *air/film/substrate/air*, but with the “absolute” reflectance given by (10), which does not properly fit the measured reflectance  $R(\lambda)$ , as explained below. Other publications [17], differently from our non-complex approach, report a complex reflectance formula. Although in some cases it is possible to use complex double precision data types, most programming languages in standard version build complex data type through a pair of single precision real numbers. Hence, our present approach appears to be more convenient from a computational point of view. However, neither of the approaches represent accurately the measured quantities, for the following reasons.

Initially, we suppose a system of four layers, with the position of the third interface

(separating the substrate from the air) given by  $L$ . We know that  $R$ , as a function of  $L$ , is a periodic function with period  $\lambda/2s$ . This period is generally much smaller than the substrate thickness, and even smaller than the error associated with this measurement. [1] Therefore, just as done in the treatment of the transmittance, a reasonable approximation to the measured reflectance is an average over the entire period:

$$\overline{R} = \frac{2s}{\lambda} \int_L^{L+\lambda/2s} R(\lambda) dL = \frac{2s}{\lambda} \int_L^{L+\lambda/2s} \left| \frac{M_{21}}{M_{22}} \right|^2 dL \quad (14)$$

After separating the terms of  $M_{21}$  and  $M_{22}$  which depend on  $L$ , we obtain

$$\overline{R} = \frac{2s}{\lambda} \int_L^{L+\lambda/2s} \frac{I_u + S_u \sin\left(\frac{4\pi s L}{\lambda}\right) + C_u \cos\left(\frac{4\pi s L}{\lambda}\right)}{I_d + S_d \sin\left(\frac{4\pi s L}{\lambda}\right) + C_d \cos\left(\frac{4\pi s L}{\lambda}\right)} dL \quad (15)$$

where the coefficients  $I_d, S_d, C_d, I_u, S_u, C_u$  depend on  $n, \kappa, s$ . We use the software Mathematica [18] to solve the integral (15), which yields

$$\overline{R} = \frac{I_u}{\rho} + \frac{S_u S_d + C_u C_d}{\rho(\rho - I_d)} \quad (16)$$

where  $\rho = \sqrt{I_d^2 - S_d^2 - C_d^2} = \frac{4s}{x}(B - Cx + Dx^2)$ , where  $B, C$  and  $D$  have the same meaning as in (4). Substituting the coefficients and simplifying them, we finally have

$$\overline{R} = \text{Reflectance} = \frac{E - Fx + Gx^2}{B - Cx + Dx^2} \quad (17)$$

where  $E, F$  and  $G$  are given by

$$F = H - 8(s-1)^2 \left( \frac{p_0 - p_1 x + p_2 x^2}{q_0 - q_1 x + q_2 x^2} \right) \quad (18)$$

$$\begin{aligned} E &= [\kappa^2 + (n-1)^2] [\kappa^2 + (1+n)(n+s^2)] \\ H &= -[(n^2-1)(n^2-s^2) + \kappa^2(1+2n^2+\kappa^2+s^2)] 2\cos(\varphi) \\ &\quad + \kappa(1+\kappa^2+n^2)(s^2-1) 2\sin(\varphi) \\ G &= [\kappa^2 + (1+n)^2] [\kappa^2 + (n-1)(n-s^2)] \end{aligned} \quad (19)$$

$$\begin{aligned}
p_0 &= \left[ (1 + \kappa^2 - n^2)(\kappa^2 + n^2)^2 + (n^2(n^2 - 1) + \kappa^2(1 + \kappa^2 + 2n^2)) s^2 \right] \cos(\varphi) \\
&\quad - \kappa n \left( (\kappa^2 + n^2)^2 - s^2 \right) 2 \sin(\varphi) \\
p_1 &= \left[ 8s + 2(1 - \kappa^2 + n^2) \right] (\kappa^2 + n^2)^2 + 2(n^2(n^2 + 1) + \kappa^2(-1 + \kappa^2 + 2n^2)) s^2 \\
p_2 &= \left[ (1 + \kappa^2 - n^2)(\kappa^2 + n^2)^2 + (n^2(n^2 - 1) + \kappa^2(1 + \kappa^2 + 2n^2)) s^2 \right] \cos(\varphi) \\
&\quad + \kappa n \left( (\kappa^2 + n^2)^2 - s^2 \right) 2 \sin(\varphi)
\end{aligned} \tag{20}$$

$$\begin{aligned}
q_0 &= \left[ \kappa^2 + (1 + n)^2 \right] \left[ \kappa^2 + (n + s)^2 \right] \\
q_1 &= - \left[ (n^2 - 1)(n^2 - s^2) + \kappa^2(-1 + 2n^2 + \kappa^2 - s(4 + s)) \right] 2 \cos(\varphi) \\
&\quad + \kappa (\kappa^2 + n^2 - s) (1 + s) 4 \sin(\varphi) \\
q_2 &= \left[ \kappa^2 + (n - 1)^2 \right] \left[ \kappa^2 + (n - s)^2 \right]
\end{aligned} \tag{21}$$

## A The PUMA Project

For simplicity, assume that for a sequence  $[\lambda_1 - \lambda_m]$  of wavelengths the transmittance of a thin film deposited on a thick transparent substrate [of known index  $s(\lambda)$ ] has been measured  $[T^{meas}(\lambda_1) - T^{meas}(\lambda_m)]$ . The theoretical equations that relate the transmittance to the wavelength are well known.[9] The transmittance is a function of the wavelength  $\lambda$ , the thickness  $d$ , the index of refraction  $n$  and the absorption coefficient  $\alpha$  of the film, the last two optical properties being unknown functions of the wavelength. So, in principle, the problem of estimating the thickness  $d$ , the refractive index  $n(\lambda)$  and the absorption coefficient  $\alpha(\lambda)$  amounts to solve the nonlinear system of equations:

$$T^{meas}(\lambda_i) = T^{theor} [\lambda_i, d, n(\lambda_i), \alpha(\lambda_i)] \text{ for } i = 1, \dots, m$$

This system is underdetermined because it has  $m$  equations and  $2m + 1$  unknowns. In order to obtain a physically meaningful solution, some physical constraints are imposed to  $n(\lambda_i)$  and  $\alpha(\lambda_i)$ . For example,  $n(\lambda_i)$  must be convex, decreasing and bounded below by 1 (normal dispersion region). The absorption coefficient must be positive and should

exhibit a concave-convex structure. As a result, the set of admissible values of the optical parameters is drastically reduced and, instead of solving the above mentioned system of equations we need to solve the optimization problem

$$\text{Minimize } \sum_{\text{all } i} [T^{\text{meas}}(\lambda_i) - T^{\text{theor}}(\lambda_i, s, d, n(\lambda_i), k(\lambda_i))]^2 \quad (22)$$

subject to the physical constraints (see [2]). Finally, using a suitable change of variables (see [3]) the feasible set is parameterized and the constraints are eliminated. For example, the constrained optimization of  $n(\lambda) \geq 1$  can be converted to the unconstrained optimization of a variable  $v$ , with  $n(\lambda) = 1 + v^2(\lambda)$ . The original method in PUMA solves the optimization problem described above using this change of variables, by means of which it becomes an unconstrained minimization problem.

When the film is very thin, say  $d < 80$  nm, the use of physical constraints are not enough for reducing the indetermination of the parameter estimation problem. In these cases, it is necessary to impose additional constraints, even without a clear evidence that they are satisfied at the solution. The introduction of *a priori* information is quite usual in the art of solving inverse problems in mathematics and engineering.[1] The additional constraints (see [6]) take the form of functional relations with a small number of parameters. This new approach is called FFM (Functional-Form Minimization) and it is presently incorporated in the PUMA project (see [5]). Note that neither PUMA nor FFM require the existence of an interference fringe pattern or of a region of very weak absorption in the  $T$  or  $R$  spectra. This constitutes a clear advantage over envelope-like methods. See the recent review by Poelman and Smet [19] for a detailed discussion on the benefits and shortcomings of the different methods being used to extract thin film properties from transmittance data only.

### III RESULTS

As said in the introduction we applied the retrieval algorithm to the reflectance of computer generated thin films and to a real amorphous silicon film deposited onto glass. The advantage of working with computer generated films is that the ‘*true*’ response is known in advance and both the goodness and the limitations of the retrieval algorithm can be readily obtained on films having very different optical properties and/or different thickness. Moreover, the retrieval algorithm can be applied to films containing variable amounts of nu-

merically generated random or systematic errors in their transmittance and/or reflectance. This possibility allows establishing the limitations of the inversion method. Finally, consistency tests are easily applied to *gedanken* films, as done along the present research.

But, as important as they might be for *gedanken* experiments, computer generated films belong to an ideal world, in the sense that they are homogeneous, perfectly flat and plane-parallel, as well as devoid of experimental errors originating either from the deposition conditions or from the limitations of the measuring apparatus. Real films are not devoid of deviations from ideal models nor from measurement errors. On the other hand, and to partially compensate these possible deficiencies, the behavior of the optical constants of real films, although not known with precision in advance, are well established and may be guessed at with a high degree of confidence. This prior knowledge of the behavior of physically meaningful responses can be used to our advantage, as done in PUMA and FFM.

All the numerical experiments and calculations were run on a Intel Pentium III Computer with the following main characteristics: 728Mbytes of RAM, 1GHz. Codes are in Fortran77 and the compiler used was GNU Fortran 0.5.25, with the optimization option “-O3”.

Using (4 and 16), the transmittance and the reflectance of many *gedanken* films were calculated (see the Appendix) and were truncated to four significant digits. For the sake of clarity we will only consider four prototypical films. They illustrate the powerfulness and the shortcomings of the retrieval algorithms.

**Film A:** Simulates a hydrogenated amorphous silicon (a-Si:H) thin film of thickness  $d^{true} = 600$  nm deposited onto a glass substrate. See Fig. 1. The wavelength dependence of the optical constants of this, and of all other *gedanken* films, are given in the appendix. This is a well behaved film, having a well defined interference pattern in a region of almost zero absorption. It may be partially deconvoluted using envelope like methods. [9] PUMA has been used to process this film.

**Film B:** Simulates a hydrogenated amorphous germanium (a-Ge:H) thin film of thickness  $d^{true} = 600$  nm deposited onto a crystalline silicon substrate. See Fig. 2. The transmittance and the reflectance of this film occurs in a spectral region of very low absorption and, due to the small difference between the index of refraction of the film and of the substrate, the amplitude of the interference oscillation amplitude remains

very small. The film data have been deconvoluted using PUMA.

**Film C:** Simulates a metal oxide very thin film ( $d^{true} = 80$  nm) deposited onto glass. As shown in Fig. 3, the  $T$  and  $R$  spectra of the film does not display an interference pattern. Clearly the data can not be inverted using envelope like methods. The thinness of the film requires the use of FFM.

**Film D:** Same as film C, but even thinner ( $d^{true} = 40$  nm). See Fig. 4. The film data were inverted using FFM, which approaches its limit of applicability.

The results of the retrieved thickness and of the optical properties of the *gedanken* films are shown in Figs. 1-4, respectively. Tables I and II indicate the quadratic error of the minimization process of the above films (1). They also display the thickness obtained by the minimization process and the “true” thickness used to generate the reflectance data.

Besides the calculated and the retrieved transmittance and reflectance of films A-D, Figs. 1 to 4 also show the retrieved index of refraction and absorption coefficient as a function of photon energy, obtained independently from  $T$  and from  $R$  spectra. Both sets of retrieved values are compared with the “true” optical constants used to generate numerically the  $T$  and  $R$  spectra. Note that the values of the calculated  $T(\lambda)$  and  $R(\lambda)$  of the films were truncated to four significant digits

Figure 5 shows the measured transmittance and reflectance of a real a-Si:H thin film deposited onto a glass substrate [20] and the retrieved optical constants obtained from the inversion of the  $T$  and  $R$  spectra.

## IV DISCUSSION

### A Computer generated films

Figure 1 indicate that the retrieval of the thickness and of the optical properties of film A has been successful. For most of the spectral range under consideration,  $n$  has been retrieved correctly. However, at high photon energies  $n$  deviates slightly from “true” values when calculated from  $T$  data. The retrieval of the “true”  $\alpha$  occurs from the inversion of both sets of data at photon energies higher than 1.5 eV. However, small absorption coefficients down to  $1 \text{ cm}^{-1}$  are retrieved from transmittance data only.  $R$  data fail to reproduce the absorption coefficient when  $\alpha < 100 \text{ cm}^{-1}$ . As known, reflectance data are more insensitive than transmittance data to variations of absorption.

In a sense, the results obtained from the inversion of the spectral data of film B are similar to the results of the previous film, except that the retrieval of both,  $n$  and  $\alpha$  from the inversion of  $T$  and  $R$  is extremely successful. Note the perfect retrieval of the refractive index in the whole spectral range and the very good agreement between retrieved and “true”  $\alpha$  in the interval  $1 < \alpha < 100 \text{ cm}^{-1}$ . The results obtained with PUMA on these two dissimilar films indicate the goodness of the method to invert reflectance data.

Figure 3 indicate the usefulness of the FFM approach to deconvolute  $T$  and  $R$  data of very thin films. The retrieval of  $n$  in film C is perfect for both sets of spectral data. The correct absorption coefficient is retrieved for over four orders of magnitude, i.e.,  $10^6$  down to  $10^2 \text{ cm}^{-1}$ . Film D simulates the same material as film C, but its thickness is even smaller,  $d = 40 \text{ nm}$ . The  $T$  and  $R$  spectra are almost flat along almost all the considered spectral range (see Fig. 4). In spite of this, the FFM algorithm does not experience difficulties in finding the “true” thickness and in retrieving the index of refraction, although the retrieval is slightly better from  $R$  data, as expected. However, the inversion algorithm fails to retrieve the absorption coefficient for  $\alpha < 10^3 \text{ cm}^{-1}$  from  $T$  data, and for  $\alpha < 5 \cdot 10^3 \text{ cm}^{-1}$  from  $R$  data. Note, however, that we are considering a  $400 \text{ \AA}$  thick film.

The above results demonstrate that both methods, PUMA and FFM, are useful tools to deal with reflectance data. They show that, in general, reflectance data provide a better retrieval of the index of refraction whereas transmittance allows a slightly better retrieval of the absorption coefficient.

A final consideration on the retrieval algorithms. Instead of using  $T$  or  $R$  data in the minimization process (22,24), both  $T$  and  $R$  can be used to our advantage [21], i.e.,

$$\begin{aligned} \text{Minimize } \sum_{all i} \{ & [T^{meas}(\lambda_i) - T^{theor}(\lambda_i, s, d, n(\lambda_i), k(\lambda_i))]^2 + \\ & [R^{meas}(\lambda_i) - R^{theor}(\lambda_i, s, d, n(\lambda_i), k(\lambda_i))]^2 \} \end{aligned} \quad (23)$$

It is well known that using (23) the estimation of the optical constants and the thickness becomes more accurate [11]. The reasons are easy to understand. The estimation problem is essentially underdetermined. When we use, for example, transmittance data only as in (22) we reduce the degrees of freedom of the solution imposing physical constraints. However, considerable freedom remains for variations of the parameters that fit reasonably well the measured data. When reflectance and transmittance data are used together there are more

data to be fitted and, consequently, the freedom for  $n$  and  $\alpha$  variations is further reduced. On the other hand, the type of information provided by a reflectance measurement and a transmittance measurement at wavelengths where the film absorbs is essentially different. If at a given  $\lambda_i$  one draws the curves:

$$T_i^{theor} = T_i^{meas} \quad \text{and} \quad R_i^{theor} = R_i^{meas}$$

in the  $(n, \kappa)$  plane, most times, they intersect forming an angle quite different from zero. This is a graphical proof of the complementarity of both kinds of informations.

Figure 6 illustrates the point for the very thin *gedanken* film D ( $d = 40$  nm). The retrieved optical constants from  $T$  and from  $R$  data for film D are shown in Fig. 4. Using (23) the retrieved  $n$  and  $\alpha$  correspond exactly to the “true” values, as shown in Fig. 6. This very good result is beyond expectation for such a film thickness. In our opinion, however, it partly derives from the fact that it is an error-free numerical experiment, an unlikely situation with the measured spectra of a real world thin film.

## B a-Si:H thin film

Before discussing the results on a-Si:H, let us briefly reconsider reflectance measurements. The intensity of the light reflected by thin films deposited onto thick transparent substrates can be measured using single-beam or double-beam spectrophotometers in which, wavelength and photometric accuracy should be verified for a meaningful set of data. The accurate measurement of reflectance at normal incidence is always a challenge because a beam splitter is necessary to divert the reflected beam to the detector. The ensuing reduction of optical intensity represents a loss of sensitivity, especially in low signal situations. Moreover, to establish the reflectance baseline a reference mirror, which requires a frequent calibration, is needed. In the selected spectral range, a good reference mirror should possess an almost flat reflectance, with  $R$  values not too far from the reflectance of the sample. Both requirements are difficult to meet in broad spectral ranges and when fringe patterns of considerable amplitude are present. Unfortunately, this is the case of most semiconductors thin films deposited onto glass substrates.

In the optimization/retrieval process we normally use linearly interpolated equally

spaced data points. As already said, retrieval experiments performed on  $R$  spectra generated under different conditions indicate the convenience of avoiding spectral data points near the extrema of the fringe pattern. The reason is that these extreme points of the interference pattern are the most sensitive to measuring errors, particularly in cases of very low signal or when the film is rather thick. A set of more convenient data points is obtained giving a weight to the selected  $R$  values. The multiplying factor is zero for points located at the extreme of the fringe pattern and in their neighborhood, and one for the other data points. Numerical simulations show that this weighting method does not affect the goodness of the retrieval process.

The estimation problem that we wish to solve has been formulated as a nonlinear programming problem as follows:

$$\text{Minimize } \sum_{\text{all } i} w_i [R^{\text{meas}}(\lambda_i) - R^{\text{theor}}(\lambda_i, s, d, n(\lambda_i), k(\lambda_i))]^2 \quad (24)$$

subject to “constraints”. That is: the objective function (24) is a weighted sum of squares, the weights being  $w_i = 0, 1; i = 1 \dots n$ . Weightless sum of squares were used in previous papers ([3, 6]). In the present research on the use of  $R$  data, the use of different weights becomes important, as shown by numerical experiments.

The thickness of the a-Si:H film retrieved from the inversion of 100 transmittance data points in the 550-950 nm wavelength interval was 1010 nm, the quadratic error being  $7.763065 \times 10^{-05}$ . To deconvolute the  $R$  spectrum equally-spaced 120 points were considered. Out of these, the weighting procedure eliminates 42. The thickness retrieved from the  $R$  spectrum using the remaining 78 points in the same wavelength interval was 1006 nm. The agreement between the two is very good, as is the agreement between the optical constants obtained from both sets of data (see Fig. 5). These results lead us to conclude that the compact formula for the reflectance (17) is correct and that the retrieval algorithm works satisfactorily with measured  $R$  spectral data of real films.

For the real a-Si:H film under analysis the results obtained with the simultaneous inversion of the  $T$  and the  $R$  data (23) were not as good as for the numerically generated thin films. In this case the quadratic error amounted to  $1.41 \times 10^{-2}$  for an optimized thickness of 1018 nm. The retrieved optical constants  $n$  and  $\alpha$  do not differ from those

found independently from  $R$  and from  $T$  data, respectively.

## C The influence of random and systematic errors on the quality of the retrieval process in *gedanken* and real films

### C.1 Random errors

The powerfulness and limitations of the retrieval algorithms have been tested considering numerically generated films in which errors in their transmittance and in their reflectance were introduced on purpose. The test has been performed on films having different thickness and properties but, to illustrate the point we just consider the case of a *gedanken* 100 nm thick a-Si:H film deposited onto a glass substrate. As usual, the values of the calculated  $T(\lambda)$  and  $R(\lambda)$  of the film were truncated to four significant digits.

First, the test consider the influence of random noise having a linearly increasing intensity level, from zero at the beginning of the  $\lambda$  interval under consideration to a maximum value at the end of the  $\lambda$  interval. The maximum noise value is given by  $N_{max} = j \cdot 10^{-i}$ , with  $i = 1, 2, 3$  and  $j = 1, \dots, 9$ , for the different trials. In other words, the maximum noise varies between  $10^{-3}$  and 0.9.

Tables III and IV summarize the results obtained from the noisy transmittance and the noisy reflectance, respectively. They indicate that:

1. The quadratic error, i.e., the difference between the calculated and the retrieved spectra, increases as  $N_{max}$  increases, as expected. Moreover, the retrieval of the optical constants worsen as  $i$  decreases.
2. The retrieval of the film thickness (100 nm) is pretty good in all cases, as indicated. The thickness error never exceeds 6% of the true value, even with  $N_{max}$  as high as 90%.
3. In general, the film thickness and of the absorption coefficient are better retrieved from noisy  $T$  spectra than from noisy  $R$  spectra. In contrast, the inversion of  $R$  data furnishes a better index of refraction.

Summarizing, it may be concluded that the existence of some random noise in the  $T$  and  $R$  spectra does not severely affect the retrieval of the film properties. However, an increasing random noise degrades the quality of the retrieved  $n$  and  $\alpha$ .

## C.2 Systematic errors

**Slit width effects** A number of tests on the influence of systematic errors were carried on on computer generated films of thickness 1200 and 1000 nm. The main result is, as in the case of random errors, that reasonable large slits –as those needed when the signal is weak because of absorption, or because the reflected signal is very small– do not affect the retrieval of the film properties. However, when the measuring slit becomes so large as to distort seriously the  $T$  or the  $R$  pattern, the algorithms fail to retrieve the true optical constants. These findings lead us to devise a way to reduce considerably the slit effect. Roughly, it consists of considering only data points of the spectrum which are less sensitive to the effect, i.e., those data that are not in the neighborhood of the interference fringe extrema.

**Photometric accuracy and non-linear detection** The important trouble with real spectrometric reflectance measurements is rarely random noise or slit width effects, but errors in spectrometric accuracy. Spectrometric accuracy may be poor because of detector calibration failures, because the response of the system is not linear in the whole detection range, or simply because the reference mirror is not properly calibrated. In what follows we show that, under normal experimental conditions, PUMA and FFM can successfully handle these types of problems.

Let us first consider photometric accuracy. Although most commercial instruments provide a four digits figure of  $R$  data it is almost impossible to measure reflectance using a scanning spectrometric instrument to better than 0.1% absolute. In fact, most commercial instruments will achieve rather poorer figures than this. As the true response is known in advance, computer generated films allow to estimate the effects of the lack of photometric accuracy on the quality of the retrieved properties. In what follows we consider the matter for both algorithms: PUMA and FFM.

Figure 7 shows the optical constants retrieved with PUMA on film A (600 nm thick,  $\alpha$ -Si:H/glass, see Fig. 1). The 'true' values are indicated in the figure, as well as those retrieved using  $R$  data rounded off to three and to two significant digits, respectively. It is apparent from Fig. 7 that the index of refraction is perfectly retrieved using only two significant digits. The true absorption coefficient is retrieved in a three decade interval, i.e.,  $10^5 - 10^2 \text{ cm}^{-1}$  using 3 and 2 significant digits of the  $R$  data. The retrieved film thickness

is 600 nm in both cases. In fact, a careful comparison between Figs. 1 and 7 indicate that the retrieval of the film properties is not worse using 3, or even 2, digit data, instead of 4. This surprising result derives from the way the algorithm uses to invert  $R$  data. Similar results were obtained with FFM when dealing with the reflectance data of the *gedanken* very film C (80 nm thick, metal oxide/glass, see Fig. 4). Figure 8 shows the retrieved optical constants as the photometric accuracy worsen, the retrieved film thickness being 80 nm in all cases. Again, the optical inversion of the  $R$  spectrum is not much worse using 2 significant digit data instead of 4 (compare Figs. 4 and 8). FFM then, can also handle this type of photometric accuracy problems in the measurement of very thin films.

Figure 9 shows the powerfulness of the inversion algorithm in a situation where both photometric accuracy and lack of linear response of the detection system are present simultaneously. We consider the output of the measured reflectance spectrum of the real a-Si:H/glass structure (see Fig. 5). As already said the measuring system delivers 4 digit  $R$  spectral data. Needless to say that in this case there is no *true* answer known in advance. The useful comparison here is between the retrieved optical properties using the full output of the measuring system and rounded off  $R$  data belonging to a selected detection range. Figure 9 displays the results of inverting  $R$  data measured in the 25-55% reflectance interval rounded off to three and to two significant digits. The strategy of the calculation is to simulate a situation in which: a) the measuring system is known to be linear in the 25-55% range, i.e., a range of reliable output data and, b) the accuracy of the detection system is not good enough. Once more, the retrieval of  $n$  is perfect and does not depend on using 3 and 2 significant digit data. In both cases the retrieved  $n$  data overlap those found from the use of the full spectrum. Similarly, the absorption coefficient is retrieved in a two decade range, i.e.,  $\approx 10^5 - 10^3 \text{ cm}^{-1}$ , as was the case with the use of the full spectral  $R$  data. Remember that the retrieval of  $\alpha$  is better using  $T$  than  $R$  data. From rounded off  $R$  data, the retrieved film thickness is 1000 nm, in good agreement with  $d = 1006$  nm obtained from the as-measured data. The above results indicate that PUMA and FFM are successful in retrieving thin film properties from reflectance data using not very accurate spectral data which may belong to a specified detection range only.

### **Systematic errors originating from an inaccurate reference mirror calibration**

Finally, we address the problem of a poorly calibrated reference mirror producing a systematic bias error in the measured  $R$  data. Normally, this frequent problem makes almost

impossible to extract the properties of very thin films from photometric measurements. To establish the powerfulness and the limitations of the present methods to deal with systematically biased  $R$  data, simulated biased  $R$  spectra of films A (Fig. 1) and C (Fig. 3) will be inverted using the PUMA and the FFM algorithms, respectively. In the numerical experiments to follow, we consider the case of a reflectance baseline mirror giving  $R$  data high along the whole wavelength range. In other words, before inversion, the true reflectance spectra will be rigidly shifted up numerically by increasing  $\Delta R$  values: 0.1%, 0.2%, 0.5% and 1.0%. The simulated biased and erroneous spectra are built as follows. *First*, the reflectance (17) is calculated as in previous sections using the thickness and the optical constants of the films (see Appendix). *Second*, the computer generated  $R$  data are rounded off to three significant digits. *Third*, the reflectance data are increased by  $\Delta R$  in the whole spectral range. *Fourth*, the erroneous  $R + \Delta R$  spectra are inverted using the PUMA (film A) or the FFM (film C) algorithms. Finally, the retrieved thickness and optical constants are compared with the “true” values used to generate the error free  $R$  spectra. Before showing the results let us anticipate that PUMA and FFM can deal with the problem of a biased set of  $R$  data in a satisfactorily way.

We consider first the quality of the film thickness retrieval from  $R + \Delta R$  spectra as a function of an increasing  $\Delta R$ . Table V shows for both films the thickness retrieved from the erroneous spectra and the quadratic error of the minimization process, the true thickness being 600 nm for film A and 80 nm for film C (see Table V). As  $\Delta R$  increases, the retrieved thickness decreases. Note that for a  $\Delta R \leq 0.1\%$  the true  $d$  is retrieved in film A and, instead of 80 nm,  $d=79$  nm is found for film C. Table V shows that as the simulated up shift  $\Delta R$  increases the retrieved thickness decreases, although not in a catastrophic way. For a 1.0%  $\Delta R$  bias,  $d = 585$  nm is found for film C, a 2% relative error. For the very thin film C, a 0.5%  $\Delta R$  bias results in a  $\Delta d/d^{true}$  of 3.75%. Numerical experiments show that the inverse situation, i.e., the deconvolution of  $R - \Delta R$  spectra, produces an increasing film thickness as  $\Delta R$  increases.

Figures 10 and 11 compare, respectively, the optical constants of films A and C retrieved from  $R + \Delta R$  spectra and their true values. It is apparent from the figures that: *i*) the index of refraction is well retrieved in all cases, even when the reflectance is high by as much as 1%; *b*) the absorption coefficient is also well retrieved for high photon energies. In the nearly transparent region of the spectra the retrieval algorithm interprets the increased

reflectance  $\Delta R$  as an increased absorption. The higher  $\Delta R$  the higher the absorption retrieved in the quasi transparent region of the spectra, as shown in Figs. 10 and 11.

Systematic, but relatively small  $\Delta R$  values, do not affect the value of the retrieved index of refraction, essentially given by the maxima of the interference  $R$  pattern in the semi-transparent region of the spectrum. When the absorption is small, say  $\alpha d < 0.01$ , the optical thickness  $nd$  of the film is related to the energy difference between  $R$  extrema that does not change with small  $\Delta R$  variations. This is the reason why  $d^{retr.} \approx d^{true}$  in Table V.

The results of Figs. 10 and 11 and Table V indicate that the retrieval algorithms PUMA and FFM are not easily fooled by an inaccurate reference mirror calibration. We think this to be one of the assets of the present contribution. Why is this so? We believe that the powerfulness of the methods derives from the philosophy of minimization. PUMA and FFM always look for the optical properties and the thickness that minimize the difference between the measurement and the calculation along the *whole* spectrum. It is clear that increasing errors, either random or systematic, result in an increasing quadratic error of the minimization process determining the best solution, as shown in Tables III, IV and V. Nonetheless, the present results indicate that for a quite broad error range the algorithms always find a solution which is near the true one, i.e., a *reasonable* solution.

## V CONCLUSIONS

In this work we present a compact formula for the reflectance of a thin film deposited on a transparent thick substrate. Two methods: PUMA, for films having a thickness in excess of 100 nm and, FFM, for very thin films ( $d < 100$  nm), were applied successfully for the retrieval of the thickness  $d$  and of the optical constants  $n, \alpha$  from reflectance data. These data were compared with values obtained from transmittance data in the same photon energy interval. The results confirm the correctness of the compact formula for  $R$  and the goodness of the retrieval algorithms. The usefulness of the inversion methods was tested on numerically generated thin films and on an a-Si:H layer deposited onto glass. *Gedanken* films indicate that, in general, reflectance data provides a better retrieval of the refractive index whereas the absorption coefficient obtained from transmittance spectra fits better the values of  $\alpha$  used to generate the spectra. The inversion of *gedanken* spectra containing variable amounts of random and of systematic errors allowed us to determine the

possibilities and limitations of the retrieval algorithms. The FFM method was successful for the mathematical inversion of the  $R$  spectrum of a 40 nm thick *gedanken* film. The simultaneous minimization of both the  $T$  and the  $R$  spectra retrieves the true optical constants of this very thin *gedanken* film.

The measurement of the reflectance of real films at normal incidence is always a real challenge, in the sense that beam splitters are necessary to divert the reflected beam to the detector and that a calibrated reference mirror is always necessary. Numerical experiments indicate the convenience of avoiding the use of  $R$  data near the extreme points of the interference fringe pattern. A method to eliminate such potentially conflicting data was implemented and successfully applied to the spectral  $R$  data of an a-Si:H film. The agreement between the results of the computational inversion of  $T$  and  $R$  data confirms the goodness of the approach.

A series of tests with  $R$  data rounded off to three and to two significant digits indicate that both PUMA and FFM can handle the problem of the lack of data accuracy in a satisfactory way. The optical inversion is also well performed in cases where the linearity of the detection system is guaranteed only in a limited detection range.

Finally, the powerfulness of the methods was tested in cases where the reference mirror produces systematic (high or low) biased data. The results on *gedanken* films demonstrate the goodness of the retrieval in cases where the systematic bias amounts to values as high as 1%. The PUMA and the FFM deconvolution algorithms are not easily mistaken by these erroneous data and always retrieve the most reasonable solution, i.e., the retrieved film properties are close to the ones used to generate the  $R$  spectra.

## **A Acknowledgments**

This work was supported by the Brazilian agencies FAPESP and CNPq. The authors are indebted to Prof. R. W. Collins and G. Ferreira (University Park, PA) for providing the measured  $T$  and  $R$  spectra of the a-Si:H thin film and for illuminating discussions regarding the challenge of measuring reflectance spectra at normal incidence.

## Appendix

Analytical expressions used to compute the substrate are

$$s_{glass}(\lambda) = \sqrt{1 + (0.7568 - 7930/\lambda^2)^{-1}} \quad (25)$$

$$s_{Si}(\lambda) = 3.71382 - 8.69123 \cdot 10^{-5}\lambda - 2.47125 \cdot 10^{-8}\lambda^2 + 1.04677 \cdot 10^{-11}\lambda^3 \quad (26)$$

For the gedanken semiconductor and dielectric films, the analytical expressions of the simulated optical constants are

a-Si:H

*Index of refraction,*

$$n^{true}(\lambda) = \sqrt{1 + (0.09195 - 12600/\lambda^2)^{-1}} \quad (27)$$

*Absorption coefficient,*

$$\ln(\alpha^{true}(E)) = \begin{cases} 6.5944 \cdot 10^{-6} \exp(9.0846E) - 16.102 & 0.60 < E < 1.40 \\ 20E - 41.9 & 1.40 < E < 1.75 \\ \sqrt{59.56E - 102.1} - 8.391 & 1.75 < E < 2.29 \end{cases} \quad (28)$$

a-Ge:H

*Index of refraction,*

$$n^{true}(\lambda) = \sqrt{1 + (0.065 - 15000/\lambda^2)^{-1}} \quad (29)$$

*Absorption coefficient,*

$$\ln(\alpha^{true}(E)) = \begin{cases} 6.5944 \cdot 10^{-6} \exp(13.629E) - 16.102 & 0.48 < E < 0.93 \\ 30E - 41.9 & 0.93 < E < 1.17 \\ \sqrt{89.34E - 102.1} - 8.391 & 1.17 < E < 1.50 \end{cases} \quad (30)$$

Metal Oxide

*Index of refraction,*

$$n^{true}(\lambda) = \sqrt{1 + (0.3 - 10000/\lambda^2)^{-1}} \quad (31)$$

*Absorption coefficient,*

$$\ln(\alpha^{true}(E)) = \begin{cases} 6.5944 \cdot 10^{-6} \exp(4.0846E) - 11.02 & 0.5 < E < 3.5 \end{cases} \quad (32)$$

**Table I:** Retrieved thicknesses and quadratic errors obtained with PUMA (using *reflectance* data) for the computer-generated films A and B.

Film	$d^{true}$	$d^{retr}$	Quadratic Error
A	600	600	$6.28 \times 10^{-4}$
B	600	600	$7.65 \times 10^{-8}$

**Table II:** Retrieved thicknesses and quadratic errors obtained with FFM (using *reflectance* data) for the computer-generated films C and D.

Film	$d^{true}$	$d^{retr}$	Quadratic Error
C	80	80	$4.50 \times 10^{-5}$
D	40	40	$1.13 \times 10^{-4}$

**Table III:** Retrieved thicknesses and quadratic errors obtained with PUMA from the noisy *transmittance* spectra of a *gedanken* a-Si:H film.

$i$	$d^{retr}$			Quadratic Error		
	1	2	3	1	2	3
$j = 1$	100	100	100	$1.4 \times 10^{-2}$	$2.6 \times 10^{-4}$	$1.0 \times 10^{-4}$
$j = 2$	101	100	100	$5.8 \times 10^{-2}$	$5.9 \times 10^{-4}$	$1.1 \times 10^{-4}$
$j = 3$	101	100	100	$1.3 \times 10^{-1}$	$1.1 \times 10^{-3}$	$1.1 \times 10^{-4}$
$j = 4$	98	100	100	$2.3 \times 10^{-1}$	$2.0 \times 10^{-3}$	$1.1 \times 10^{-4}$
$j = 5$	101	100	100	$3.7 \times 10^{-1}$	$3.9 \times 10^{-3}$	$1.2 \times 10^{-4}$
$j = 6$	100	100	100	$4.8 \times 10^{-1}$	$4.9 \times 10^{-3}$	$1.2 \times 10^{-4}$
$j = 7$	102	100	100	$7.6 \times 10^{-1}$	$7.7 \times 10^{-3}$	$1.4 \times 10^{-4}$
$j = 8$	95	100	100	$7.3 \times 10^{-1}$	$7.6 \times 10^{-3}$	$2.0 \times 10^{-4}$
$j = 9$	101	100	100	$1.4 \times 10^{-1}$	$1.1 \times 10^{-2}$	$1.7 \times 10^{-4}$

**Table IV:** Retrieved thicknesses and quadratic errors obtained with PUMA from the noisy *reflectance* spectra of a *gedanken* a-Si:H film.

$i$	$d^{retr}$			Quadratic Error		
	1	2	3	1	2	3
$j = 1$	99	100	100	$1.2 \times 10^{-2}$	$1.4 \times 10^{-4}$	$1.2 \times 10^{-5}$
$j = 2$	99	100	100	$5.7 \times 10^{-2}$	$4.7 \times 10^{-4}$	$1.6 \times 10^{-5}$
$j = 3$	98	100	100	$1.2 \times 10^{-1}$	$1.2 \times 10^{-3}$	$2.4 \times 10^{-5}$
$j = 4$	100	100	100	$2.1 \times 10^{-1}$	$1.8 \times 10^{-3}$	$2.7 \times 10^{-5}$
$j = 5$	103	100	100	$3.7 \times 10^{-1}$	$3.5 \times 10^{-3}$	$6.1 \times 10^{-5}$
$j = 6$	100	100	100	$5.7 \times 10^{-1}$	$4.3 \times 10^{-3}$	$5.6 \times 10^{-5}$
$j = 7$	105	100	100	$6.6 \times 10^{-1}$	$5.9 \times 10^{-3}$	$7.3 \times 10^{-5}$
$j = 8$	102	100	100	$9.7 \times 10^{-1}$	$7.9 \times 10^{-3}$	$9.6 \times 10^{-5}$
$j = 9$	94	99	100	$1.0 \times 10^{-1}$	$1.1 \times 10^{-2}$	$1.1 \times 10^{-4}$

**Table V:** Retrieved thicknesses and quadratic errors obtained with PUMA and FFM, respectively, from the deconvolution of the rigidly shifted *reflectance* spectra of the *gedanken* films A and C.

Film A ( $d = 600\text{nm}$ )

$\Delta R$	retr. thickness	Quad. error
0.1%	600	$1.06 \times 10^4$
0.2%	597	$1.24 \times 10^4$
0.3%	595	$1.57 \times 10^4$
0.4%	596	$2.49 \times 10^4$
0.5%	592	$2.69 \times 10^4$
0.6%	591	$3.63 \times 10^4$
0.7%	598	$4.52 \times 10^4$
0.8%	590	$6.54 \times 10^4$
1%	586	$9.59 \times 10^4$

Film C ( $d = 80\text{nm}$ )

0.1%	79	$7.10 \times 10^4$
0.2%	79	$1.09 \times 10^3$
0.5%	77	$7.77 \times 10^4$

## References

- [1] I. Chambouleyron and J. M. Martínez, in *Handbook of Thin Films Materials*, edited by H. S. Nalwa. Volume **3**, Ch. 12 (Academic Press, San Diego, 2001), pp. 593-622.
- [2] I. Chambouleyron, J. M. Martínez, A. C. Moretti and M. Mulato, *Appl. Optics* **36**, pp. 8238–8247 (1997).
- [3] E. G. Birgin, I. Chambouleyron and J. M. Martínez, *J. Comp. Phys.* **151**, pp. 862–880 (1999).
- [4] M. Mulato, I. Chambouleyron, E. G. Birgin and J. M. Martínez, *Appl. Phys. Letters.* **77**, pp. 2133–2135 (2000).
- [5] [www.ime.unicamp.br/~puma](http://www.ime.unicamp.br/~puma)
- [6] I. Chambouleyron, S. Ventura, E. G. Birgin and J. M. Martínez, *J. Appl. Phys.* **92**, pp. 3093-3102 (2002).
- [7] E. G. Birgin, I. Chambouleyron, J. M. Martínez and S. Ventura, *Appl. Numerical Math.* **47**, 109-119 (2003).
- [8] M. Raydan, *SIAM J. Optim.* **7**, pp. 26–33 (1997).
- [9] R. Swanepoel, *J. Phys. E: Sci. Instrum.* **16**, pp. 1214–1222 (1983).
- [10] M. Born and E. Wolf, *Principles of Optics* (6<sup>th</sup> ed. Pergamon Press, UK, 1993).
- [11] O. S. Heavens, *Optical Properties of Thin Solid Films* (Dover Pub., New York, 1991).
- [12] R. D. Bringans, *J. Phys. D: Appl. Phys.* **10**, pp. 1855–1861 (1977).
- [13] R. E. Denton, R. D. Campbell, S. G. Tomlin, *J. Phys. D: Appl. Phys.* **5**, pp. 852–863 (1972).
- [14] G. Hass, R. E. Thun, in *Physics of Thin Films* (Academic Press, 1969).
- [15] P. O. Nilsson, *Appl. Optics* **7**, pp. 435–442 (1968).
- [16] C. Reale, *Thin Solid Films* **9**, pp. 395–407 (1972)
- [17] Y. Hishikawa, N. Nakamura, S. Tsuda, S. Nakano, Y. Kishi, Y. Kuwano, *Jap. J. Appl. Phys.* **30**, pp. 1008–1014 (1991).

[18] [www.wolfram.com](http://www.wolfram.com)

[19] D. Poelman and P. F. Smet, *J. Phys. D: Appl. Phys.* **36**, 1850-1857 (2003)

[20] The measured  $T$  and  $R$  spectral data contain 4 digits. The authors are indebted to Prof. R. Collins and G. Ferreira, University Park, PA, for careful measurements of the transmittance and the reflectance spectra of the a-Si:H film reported in the present work. The authors also thanks Prof. Collins for illuminating discussions regarding measuring techniques.

[21] T. C. Paulick, *Appl. Optics* **25**, pp. 562–564 (1986).

## VI FIGURE CAPTIONS

**Figure 1:** ‘*True*’ (dashed lines) and retrieved transmittance (filled circles), reflectance (open circles) and optical constants from  $T$  and  $R$  (film A, PUMA). Note that the retrieval from  $R$  gives a slightly better index of refraction whereas the absorption coefficient is better retrieved from the transmittance spectrum.

**Figure 2:** ‘*True*’ (dashed lines) and retrieved transmittance (filled circles), reflectance (open circles) and optical constants from  $T$  and  $R$  (film B, PUMA). Note that the index of the film and of the substrate have close values. As a consequence the amplitude of the interference oscillation is rather small. In this case the optical constants are retrieved with a similar degree of accuracy.

**Figure 3:** ‘*True*’ (dashed lines) and retrieved transmittance (filled circles), reflectance (open circles) and optical constants from  $T$  and  $R$  (very thin film C, FFM). The optical constants of this very thin film are retrieved from both  $T$  and  $R$  spectra. However, the absorption coefficient is better retrieved from transmittance data.

**Figure 4:** ‘*True*’ (dashed lines) and retrieved transmittance (filled circles), reflectance (open circles) and optical constants from  $T$  and  $R$  (very thin film D, FFM). Note that the thickness  $d = 40$  nm has been equally retrieved from  $T$  and  $R$ . The index of refraction is pretty well retrieved but the absorption coefficient is found for values in excess of  $10^4$   $\text{cm}^{-1}$ .

**Figure 5:** Top: Measured and retrieved transmittance and reflectance of an  $a$ -Si:H film deposited onto glass. Bottom: Retrieved optical constants from the  $T$  (filled circles) and from the  $R$  (open circles) spectra. The agreement between the two is very good, as is the retrieved thickness. As in the case of gedanken films, the retrieval of  $\alpha(\lambda)$  is better from the  $T$  spectrum.

**Figure 6:** Retrieval of the optical constants of the very thin film D ( $d = 40$  nm) minimizing both,  $T$  and  $R$  simultaneously (23). Note the perfect agreement between retrieved and ‘*true*’ values, even at very small  $\alpha$ .

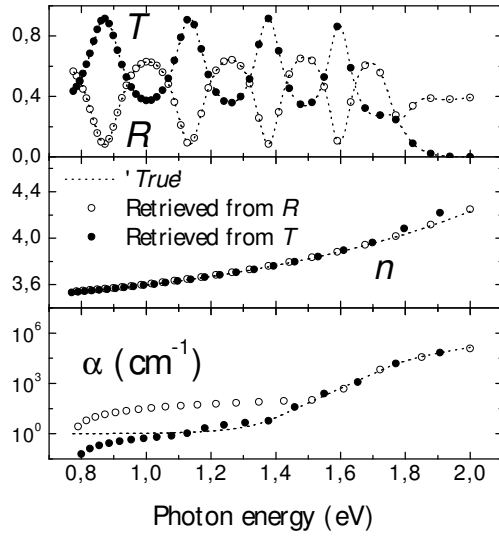
**Figure 7:** ‘*True*’ (dashed lines) and retrieved optical constants of film A (PUMA). Open squares:  $R$  data rounded off to three digits; open circles:  $R$  data rounded off to two digits.

**Figure 8:** ‘True’ (dashed lines) and retrieved optical constants of film C (FFM). Open squares:  $R$  data rounded off to three digits; open circles:  $R$  data rounded off to two digits.

**Figure 9:** Retrieved data from the as-measured reflectance spectrum of an  $a$ -Si:H thin film (dashed lines, same as Fig. 5) and retrieved optical constants using rounded off data. Open squares:  $R$  data rounded off to three digits; open circles:  $R$  data rounded off to two digits. The rounded off data were taken from a selected detection amplitude interval, i.e.,  $25\% < R < 55\%$ .

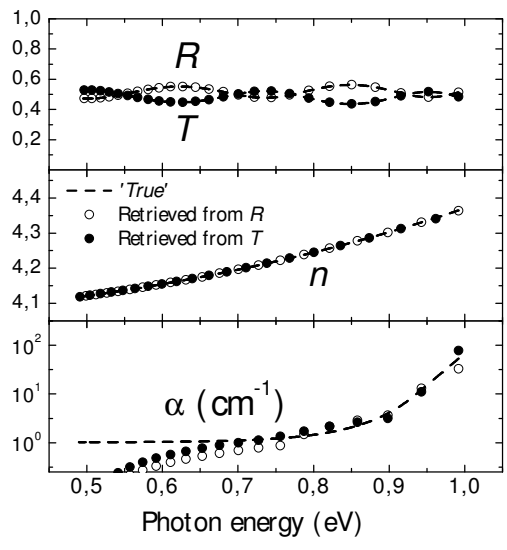
**Figure 10:** Dashed line - ‘true’ values of the optical constants of film A. Open symbols: retrieved optical constants from  $R + \Delta R$  spectra. Circles:  $\Delta R = 0.2\%$ ; squares  $\Delta R = 1\%$ .

**Figure 11:** Dashed line - ‘true’ values of the optical constants of film C. Open symbols: retrieved optical constants from  $R + \Delta R$  spectra. Circles:  $\Delta R = 0.1\%$ ; squares  $\Delta R = 0.5\%$ .



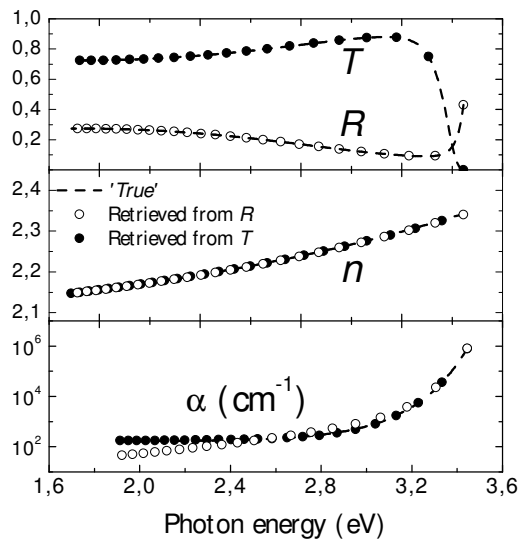
Ventura et al

JR04 – 1629, Fig. 1/11



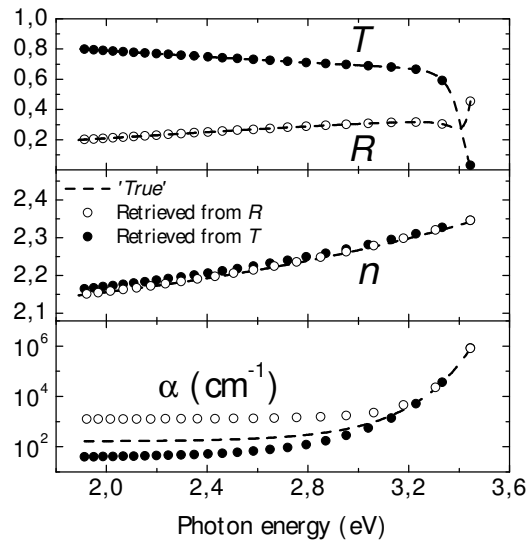
Ventura et al

JR04 – 1629, Fig. 2/11



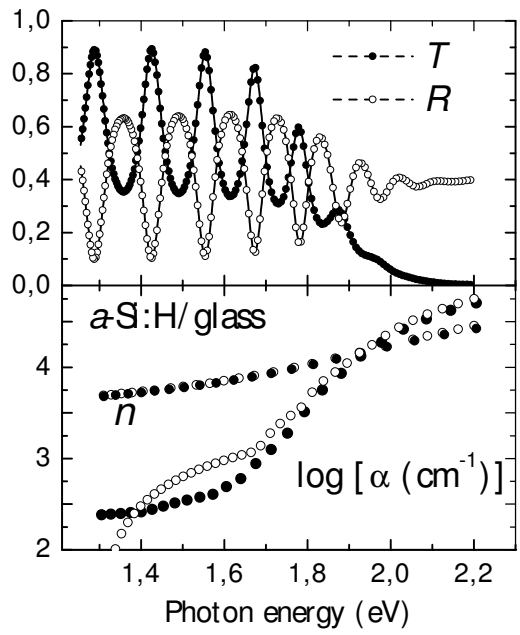
Ventura et al

JR04 – 1629, Fig. 3/11



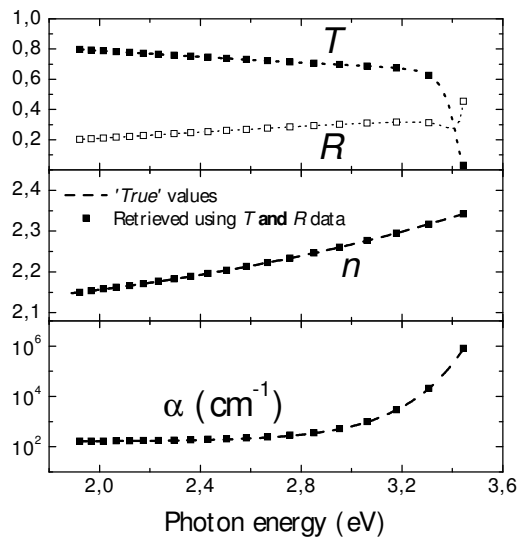
Ventura et al

JR04 – 1629, Fig. 4/11



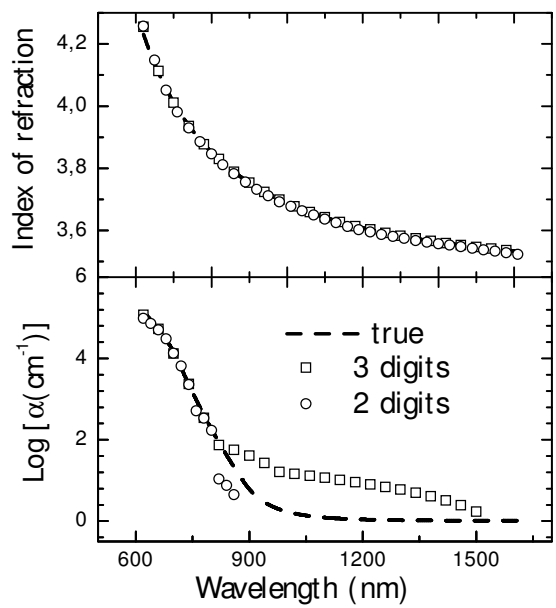
Ventura et al

JR04 – 1629, Fig. 5/11



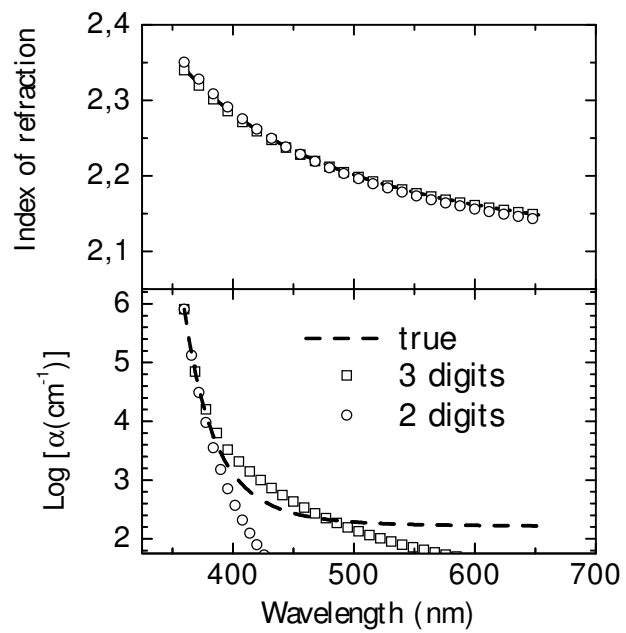
Ventura et al

JR04 – 1629, Fig. 6/11



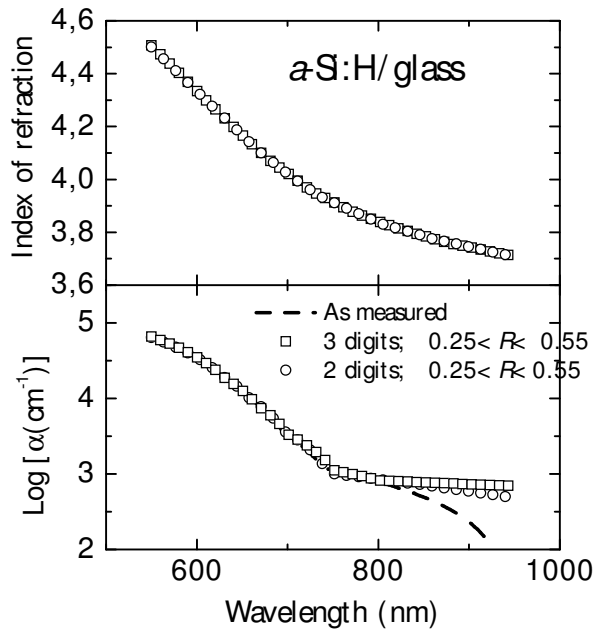
Ventura et al

JR04 – 1629, Fig. 7/11



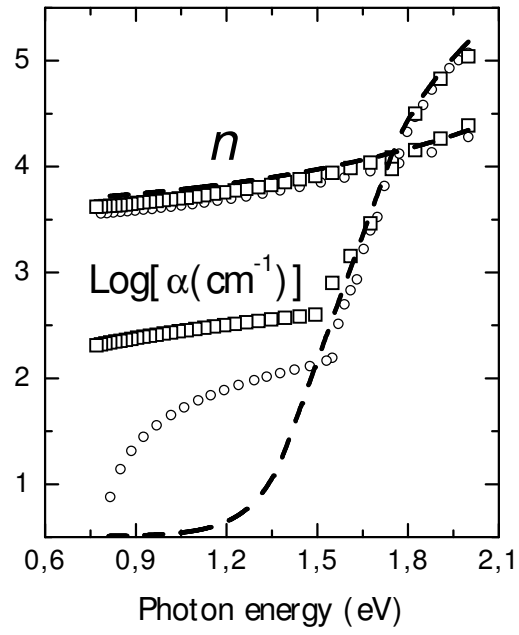
Ventura et al

JR04 – 1629, Fig. 8/11



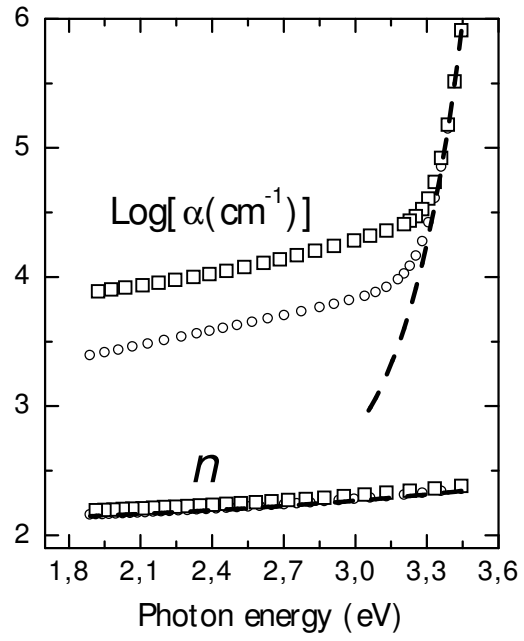
Ventura et al

JR04 – 1629, Fig. 9/11



Ventura et al

JR04 – 1629, Fig. 10/11



Ventura et al

JR04 – 1629, Fig. 11/11